



Published in final edited form as:

Cancer Discov. 2012 July ; 2(7): 638–651. doi:10.1158/2159-8290.CD-12-0093.

## The Transcription Factor ZNF217 Is a Prognostic Biomarker and Therapeutic Target during Breast Cancer Progression

Laurie E. Littlepage<sup>1,2</sup>, Adam S. Adler<sup>3</sup>, Hosein Kouros-Mehr<sup>1</sup>, Guiqing Huang<sup>1,2</sup>, Jonathan Chou<sup>1,2</sup>, Sheryl R. Krig<sup>4</sup>, Obi L. Griffith<sup>5</sup>, James E. Korkola<sup>5</sup>, Kun Qu<sup>3</sup>, Devon A. Lawson<sup>1,2</sup>, Qing Xue<sup>1</sup>, Mark D. Sternlicht<sup>1,2</sup>, Gerrit J. P. Dijkgraaf<sup>1</sup>, Paul Yaswen<sup>5</sup>, Hope S. Rugo<sup>2</sup>, Colleen A. Sweeney<sup>4</sup>, Colin C. Collins<sup>2</sup>, Joe W. Gray<sup>2,5</sup>, Howard Y. Chang<sup>3,6</sup>, and Zena Werb<sup>1,2</sup>

<sup>1</sup>Department of Anatomy, University of California, San Francisco <sup>2</sup>Helen Diller Family Comprehensive Cancer Center, University of California, San Francisco <sup>3</sup>Program in Epithelial Biology, Stanford University School of Medicine, Stanford <sup>4</sup>Division of Basic Sciences, University of California at Davis Cancer Center, Sacramento <sup>5</sup>Life Sciences Division, Lawrence Berkeley National Laboratory, Berkeley, California <sup>6</sup>Howard Hughes Medical Institute, Chevy Chase, Maryland

### Abstract

The transcription factor ZNF217 is a candidate oncogene in the amplicon on chromosome 20q13 that occurs in 20% to 30% of primary human breast cancers and that correlates with poor prognosis. We show that *Znf217* overexpression drives aberrant differentiation and signaling events, promotes increased self-renewal capacity, mesenchymal marker expression, motility, and metastasis, and represses an adult tissue stem cell gene signature downregulated in cancers. By *in silico* screening, we identified candidate therapeutics that at low concentrations inhibit growth of cancer cells expressing high ZNF217. We show that the nucleoside analogue triciribine inhibits ZNF217-induced tumor growth and chemotherapy resistance and inhibits signaling events [e.g.,

© 2012 American Association for Cancer Research.

Corresponding Author: Zena Werb, Department of Anatomy, University of California, Box 0452, 513 Parnassus Avenue, San Francisco, CA 94143. Phone: 415-476-4622; Fax: 415-476-4565; zena.werb@ucsf.edu.

Current address for A.S. Adler, H. Kouros-Mehr, and G.J.P. Dijkgraaf: Genentech, South San Francisco, CA 94080; current address for M.D. Sternlicht: FibroGen, 409 Illinois Street, San Francisco, CA 94158; current address for C.C. Collins: The Vancouver Prostate Centre, Vancouver, BC V5Z 1M9, Canada; and current address for J.W. Gray: Department of Biomedical Engineering, Oregon Health and Science University, Portland, OR 97239.

### Disclosure of Potential Conflicts of Interest

J.W. Gray has a Commercial Research Grant from GlaxoSmith-Kline, Pfizer and Susan G. Komen and is a consultant/advisory board member for New Leaf Ventures, Agendia, and KromaTiD. No potential conflicts of interests were disclosed by the other authors.

**Note:** Supplementary data for this article are available at Cancer Discovery Online (<http://cancerdiscovery.aacrjournals.org/>).

### Authors' Contributions

**Conception and design:** L.E. Littlepage, H. Kouros-Mehr, D.A. Lawson, H.S. Rugo, Z. Werb

**Development of methodology:** L.E. Littlepage, H. Kouros-Mehr, G. Huang, S.R. Krig, O.L. Griffith, D.A. Lawson, Z. Werb

**Acquisition of data (provided animals, acquired and managed patients, provided facilities, etc.):** L.E. Littlepage, A.S. Adler, J. Chou, S.R. Krig, J.E. Korkola, D.A. Lawson, Q. Xue, C.C. Collins, Z. Werb

**Analysis and interpretation of data (e.g., statistical analysis, biostatistics, computational analysis):** L.E. Littlepage, A.S. Adler, J. Chou, O.L. Griffith, J.E. Korkola, K. Qu, D.A. Lawson, M.D. Sternlicht, H.S. Rugo, C.A. Sweeney, H.Y. Chang, Z. Werb

**Writing, review, and/or revision of the manuscript:** L.E. Littlepage, H. Kouros-Mehr, J. Chou, O.L. Griffith, J.E. Korkola, K. Qu, G.J.P. Dijkgraaf, P. Yaswen, H.S. Rugo, C.A. Sweeney, C.C. Collins, J.W. Gray, H.Y. Chang, Z. Werb

**Administrative, technical, or material support (i.e., reporting or organizing data, constructing databases):** L.E. Littlepage, C.A. Sweeney, Z. Werb

**Study supervision:** L.E. Littlepage, Z. Werb

**Made reagents available before they were published:** G.J.P. Dijkgraaf

phospho-AKT, phospho-mitogen-activated protein kinase (MAPK)] *in vivo*. Our data suggest that ZNF217 is a biomarker of poor prognosis and a therapeutic target in patients with breast cancer and that triciribine may be part of a personalized treatment strategy in patients overexpressing ZNF217. Because ZNF217 is amplified in numerous cancers, these results have implications for other cancers.

**SIGNIFICANCE**—This study finds that ZNF217 is a poor prognostic indicator and therapeutic target in patients with breast cancer and may be a strong biomarker of triciribine treatment efficacy in patients. Because previous clinical trials for triciribine did not include biomarkers of treatment efficacy, this study provides a rationale for revisiting triciribine in the clinical setting as a therapy for patients with breast cancer who overexpress ZNF217.

## INTRODUCTION

In the most aggressive breast tumors, neoplastic cells activate or amplify oncogenes or inactivate or delete tumor suppressor genes to promote invasive growth and poor prognosis in patients. Amplification of the human chromosomal region 20q13 occurs in 20% to 30% of primary human breast cancers, as well as in other cancers, and its amplification correlates with poor patient prognosis (1, 2).

The ZNF217 gene on human 20q13.2 encodes a transcription factor that is overexpressed in all breast tumors and cell lines in which the gene is amplified, as compared with normal mammary tissue and epithelial cells (1, 2). The ZNF217 protein is a member of the C<sub>2</sub>H<sub>2</sub> family of transcription factors and contains 8 predicted Kruppel-like C<sub>2</sub>H<sub>2</sub> zinc finger motifs and a proline-rich region. It is a component of a human histone deacetylase complex (CoREST-HDAC) and is found in complexes with the transcriptional co-repressor C-terminal binding protein (CtBP), the histone demethylases LSD1 (H3K4, H3K9) and KDM5B/JARID1B/PLU-1 (H3K4), and the methyltransferases G9a (H3K9, H3K27) and EZH2 (H3K27; refs. 3–8). Its overexpression in human mammary epithelial cells (MEC) overcomes senescence and promotes immortalization accompanied by increased telomerase activity, increased resistance to TGFβ-induced growth inhibition, and amplification of *c-MYC* (9). ZNF217 binds to the promoters of genes involved in differentiation and is repressed following retinoic acid treatment of pluripotent embryonal cells (10).

In this study, we investigated whether and how ZNF217 promotes tumor progression and poor prognosis using cultured cells, *in vivo* transplant models, and human patient expression data sets.

## RESULTS

### ZNF217 Is Prognostic of Poor Survival in Breast Cancer Patients

Using microarray expression data from primary breast tumors and corresponding clinical data (11, 12), we found that high ZNF217 amplification and expression correlate with shorter overall, disease-specific, and relapse-free survival (Fig. 1A and B; Supplementary Fig. S1A and S1B). To determine whether ZNF217 overexpression overlapped with another poor prognostic subtype, we compared ZNF217 expression levels across patient subtypes [e.g., estrogen receptor (ER)<sup>+</sup>, ER<sup>-</sup>, ERBB2/HER2<sup>+</sup>, EPBB2/HEP2<sup>-</sup>, luminal, and basal patient cohorts] and found that ZNF217 expression levels are highest in ER<sup>+</sup> tumors and lowest in basal subtype tumors (data not shown).

We next determined whether ZNF217 had prognostic value across breast cancer subtypes. We compared survival and ZNF217 expression by univariate analysis across ER<sup>+</sup>, ER<sup>-</sup>, HER2<sup>+</sup>, luminal, and basal subtypes. Patients with tumors expressing high ZNF217 consistently had reduced survival compared with patients with tumors expressing lower

*ZNF217* across multiple breast cancer subtypes (Fig. 1C and data not shown). For example, in a meta-analysis of relapse-free survival across 9 published studies that included 858 patients [ER<sup>+</sup>HER2<sup>-</sup> lymph node (LN)<sup>-</sup>] with *ZNF217* expression, we found that *ZNF217* expression was significantly associated with 5-year ( $P = 0.012$ ) and 10-year ( $P = 0.023$ ) relapse status (Mann–Whitney), and patients with relapse had higher *ZNF217* expression. Similarly, patients grouped into the high-expression tertile had significantly worse survival than low-expression groups. These data show that *ZNF217* is prognostic of poor survival in patients by univariate analysis. Moreover, *ZNF217* was a better predictor of survival than ER status by multivariate analysis (Supplementary Fig. S1C).

### Overexpression of *Znf217* Accelerates Loss of Adhesion and Increased Motility in Mouse MECs

To determine the consequences of *Znf217* overexpression, we generated mouse mammary epithelial cell lines that overexpressed *Znf217* by retroviral and lentiviral infection. Mouse mammary epithelial cell lines (SCp2, NMuMG, EpH4) overexpressing *Znf217* had altered motility showing a more scattered phenotype than adherent, clustered control cells (Fig. 2A–C; Supplementary Fig. S2A–S2C). In a wound-healing/scratch assay, individual SCp2 cells (Fig. 2D) and NMuMG cells (data not shown) overexpressing *Znf217* showed increased motility, forward extended lamellipodia, and independent migration (i.e., separate from other cells) toward the middle of the scratch (Fig. 2D; Supplementary Movie S1). In contrast, vector-treated cells migrated as a sheet predominantly with a single leading edge. In keeping with the increased motility, cells overexpressing *Znf217* reorganized their actin cytoskeleton with reduced cortical actin and increased actin stress fibers (Fig. 2E) and upregulated epithelial-to-mesenchymal transition (EMT) markers including Snail1 and Twist (Fig. 2F). Consistently, we found that *ZNF217* expression levels correlated with expression of EMT markers, including *Snail1*, *Snail2*, and *Vimentin*, genes that have *ZNF217* enriched at their promoters in human breast cancer cell lines and tumors (Supplementary Table S1). Taken together, these results indicate that the early effects of increased *ZNF217* expression would lead to premalignant changes of enhanced mammary epithelial migration.

We used gene expression microarrays of the mouse SCp2 MECs overexpressing *Znf217* to identify altered processes and molecular targets of *Znf217* (Fig. 2G). In these cells, 176 genes were upregulated and 243 genes downregulated following *Znf217* overexpression. We used DAVID software to classify the gene sets with Gene Ontology (GO) terms (Supplementary Table S2). The GO terms suggested that *Znf217* overexpression promoted increased cell motility, decreased epithelial differentiation, increased vasculature development, and changes at the membrane.

We also assayed for clonogenicity and transformation potential *in vitro*. *Znf217* overexpression in NIH3T3 cells stimulated anchorage-independent growth in a soft agar assay, with increased number and size of colonies (Fig. 3A–C).

### *Znf217* Overexpression in Normal Primary Mammary Epithelium Promotes Increased Mammosphere Formation in Culture

Because we found that *Znf217* overexpression in culture promoted increased motility, decreased epithelial marker expression/increased mesenchymal marker expression, and increased clonogenicity/transformation potential *in vitro*, we reasoned that these changes were consistent with a change in differentiation toward a less differentiated or more mesenchymal phenotype. *Znf217* gene expression was enriched in the CD24<sup>Med</sup>CD49<sup>High</sup> cell population, which includes basal, myoepithelial, and progenitor cells, compared with

CD24<sup>High</sup>CD49f<sup>Low</sup> cells, which include luminal and luminal progenitor cells (Fig. 3D and E).

To determine whether ZNF217 could promote progenitor cell phenotypes, we overexpressed *Znf217* in normal primary MECs and analyzed clonogenicity potential in the mammosphere assay. Primary MECs infected with *Znf217*-overexpressing lentivirus and grown in serum-free nonadherent culture conditions showed increased self-renewal capacity (Fig. 3F and G).

### Gene Expression Analysis of MECs Following *Znf217* Overexpression Predicts Changes in Epithelial Proliferation, Cell Adhesion, and Motility

We next determined the impact of *Znf217* overexpression on global gene expression in normal primary mouse MECs by gene expression microarrays (Fig. 3H). Primary MECs were infected with a *Znf217*-overexpressing lentivirus, passaged to expand the population, and confirmed to overexpress *Znf217* by quantitative reverse transcription PCR (qRT-PCR; Fig. 3I). In these MECs, 340 genes were upregulated and 401 genes downregulated following *Znf217* overexpression (Fig. 3H). The GO terms classified by DAVID software (Supplementary Table S2) suggested that *Znf217* overexpression altered the gene expression profile of genes involved in cell proliferation, cell adhesion, cell migration, G-protein-coupled receptor signaling pathways, and ribosomal function.

Genes identified by microarray analysis suggested that overexpressing *Znf217 in vivo* would promote increased epithelial growth or progenitor cell expansion (Fig. 3H; Supplementary Table S2). These genes included a number of TGF $\beta$  and Wnt pathway genes (*Axud1/Csrnp-1, Bcl9l, Bmper, Bmpr2, follistatin, Samd9l, Sfrp1, Tcf4, Tgf $\beta$ 2, Tgf $\beta$ 3, Wnt5a*). We validated selected genes including *Wnt5a* and *Sfrp1* by qRT-PCR (Fig. 3J). These results are consistent with ZNF217 promoting differentiation toward a less differentiated cell-like phenotype via aberrant signaling in the TGF $\beta$  and Wnt pathways. We also found that ZNF217 was required for cell proliferation (Supplementary Fig. S2D).

We also examined epithelial marker expression in our microarray data set. We found increased expression of both *K17* (myoepithelial marker) and *K18* (luminal epithelial marker; Fig. 3H). Consistent with these results, we found that ZNF217 expression levels correlated with expression of *K19* and *K8/18*, genes with ZNF217 enriched at their promoters in human breast cancer cell lines and tumors and with down-regulated expression after ZNF217 knockdown in MCF7 cells (Supplementary Tables S1 and S3).

### *Znf217* Overexpression in Primary MECs Represses an Adult Stem Cell Expression Signature Downregulated in Cancers

Because the aberrant differentiation markers seen both *in vivo* and in culture suggest that ZNF217 may push MECs to a more progenitor cell-like phenotype, we compared our microarray data set expression pattern with our previously defined gene expression signature that we found expressed in adult stem cells (13). Many of these adult stem cells are slowly cycling and show balanced differentiation versus self-renewal during normal homeostasis. Adult stemness as defined by this adult stem cell signature is not correlated with self-renewal. This signature has high expression in normal tissues, where cells predominantly are quiescent and have limited self-renewal, but low expression in cancerous tissues, where cells can self-renew. Therefore, reduced expression of the signature correlates with increased self-renewal (13).

Similar to that seen in cancers, primary MECs overexpressing *Znf217* significantly repressed genes of the adult stem cell signature (Supplementary Table S4;  $P = 1.89 \times 10^{-10}$ ), thus making normal cells like self-renewing cancer cells at the expression level. Consistent

with the increased clonogenicity by mammosphere assay, this alteration in the expression signature suggests that ZNF217 may block differentiation and/or promote self-renewal.

### Tumors Overexpressing *Znf217* Have a More Basal Pathology with Increased Dual-Positive Luminal and Basal Cell Marker Expression

Our finding that *Znf217* overexpression promoted decreased differentiation in normal and immortalized mammary epithelium prompted us to determine whether these changes are also followed in tumorigenic mammary epithelium both in culture and *in vivo*. We overexpressed *Znf217* by lentiviral delivery of *Znf217* into primary luminal-type mammary epithelial tumor cells isolated from 18-week-old MMTV-PyMT mice (PyMT MEC) or an MMTV-PyMT cell line (Vo-PyMT), sorted the cells for the IRES-Tomato reporter gene, and confirmed *Znf217* overexpression by qRT-PCR (Fig. 4A). In culture, ZNF217 induced mesenchymal marker expression, reduced expression of E-cadherin, increased expression of EMT markers *Snail2* and *Twist* (Fig. 4A), and produced a more scattered phenotype (Supplementary Fig. S2C). In addition, cells overexpressing *Znf217* readily formed increased numbers of mammospheres compared with vector control cells (Fig. 4B and C).

When the sorted cells were transplanted into syngeneic mouse mammary fat pads cleared of epithelium, *Znf217* over-expression accelerated the rate of tumor formation, reduced the tumor-free survival, and increased both tumor volume and final tumor weight (Fig. 4D–F; Supplementary Fig. S3A). Tumors overexpressing *Znf217* had a markedly altered, heterogeneous histology compared with tumors from vector-treated cells (Fig. 4G). Control tumors had little to no smooth muscle actin (SMA) staining with predominantly luminal K8<sup>+</sup> epithelium, whereas *Znf217*-overexpressing tumors expressed higher levels of myoepithelial and myofibroblast SMA protein (Fig. 4H).

Tumor cells from vector-treated cohorts were predominantly K8<sup>+</sup> with few K14<sup>+</sup> cells; most of the K14<sup>+</sup> cells were K8<sup>-</sup> and were located basal to the K8<sup>+</sup> tumor cells. *Znf217* over-expression increased numbers of K14<sup>+</sup> cells in tumors, with many double-positive K8<sup>+</sup>K14<sup>+</sup> cells (Fig. 4I and J and data not shown). The K8<sup>+</sup>K14<sup>+</sup> cells may be a bipotent progenitor population capable of forming both luminal and myoepithelial cells, also seen by others as K18<sup>+</sup>K19<sup>+</sup> cells (14–18).

We also assayed for epithelial E-cadherin expression in these tumors. *In vivo* *Znf217* overexpression resulted in heterogeneous staining of E-cadherin with a large number of regions containing a marked reduction in E-cadherin expression, whereas control tumors had E-cadherin localized to the plasma membrane throughout the epithelium (Fig. 5A; Supplementary Fig. S3B).

Taken together, these phenotypic changes seen within tumors are consistent with *Znf217* promoting the acquisition of a mesenchymal/progenitor cell phenotype.

### Overexpression of *Znf217* Promotes Metastasis

Because metastasis *in vivo* often is accompanied by increased motility, invasion, and mesenchymal/basal phenotypes, we next asked whether ZNF217 promotes metastasis *in vivo*. In mice transplanted with either PyMT or Vo-PyMT cells, *Znf217* over-expression significantly increased the percentage of mice with lung metastases, increased metastatic burden, and increased the number of spontaneous lung metastases per mouse (Fig. 5B–D; Supplementary Fig. S3C). In keeping with these results, high ZNF217 expression was prognostic of reduced metastasis-free survival in patients with breast cancer (Fig. 5E; ref. 19).

## ZNF217 Promotes Resistance to Chemotherapy

Patients with tumors expressing stem cell–like/progenitor cell markers have increased resistance to chemotherapy (20). We determined whether *ZNF217* was a prognostic predictor of treatment response by comparing clinical data with expression data from patients who received neoadjuvant chemotherapy. In one data set, patients received either doxorubicin or a combination of 5-fluorouracil and mitomycin (FUMI) before surgical removal and microarray gene expression analysis of the tissue (12). Tumors that responded to treatment (i.e., became smaller) expressed less *ZNF217* than did nonresponsive tumors (Fig. 6A).

We also found that tumors with low *ZNF217* expression responded better to treatment (pathologic complete response) than did tumors with high *ZNF217* expression. In a second data set, fine needle aspirate samples were collected before treatment and used for gene expression (21). All patients received similar preoperative treatments (paclitaxel and fluorouracil-doxorubicin-cyclophosphamide). We found *ZNF217* expression levels higher in nonresponsive tumors that did not respond to therapy than in tumors that responded (Fig. 6A). Therefore, *ZNF217* is a prognostic predictor of patient outcome in response to chemotherapy.

## ZNF217 Levels Are Related to Levels of Activated AKT, Mitogen-Activated Protein Kinase, and ERBB3

ERBB3 is a direct target of *ZNF217* (22). We found significant correlation between *ZNF217* and ERBB3 expression levels in human breast tumors (Fig. 6B). To determine the mechanism underlying the effects of *ZNF217*, we analyzed several downstream signaling molecules downstream of ERBB3 in 2 human breast cancer cell lines (MCF7, ZR-75-1) that express high levels of *ZNF217*. Using both wild-type cells and cells after knockdown for *ZNF217* expression by siRNA, as described previously (22), we treated serum-starved cells with the growth factor ligand for ERBB3, heregulin/neuregulin (HRG). Cells containing *ZNF217*-siRNAs consistently required higher concentrations of heregulin to induce ERBB3 signaling, phospho-AKT, and phospho-mitogen-activated protein kinase (MAPK; Fig. 6C; Supplementary Fig. S4A–S4D). These data indicate that these pathways are downstream of *ZNF217* and that *ZNF217* sensitizes cells to heregulin.

## ZNF217 Is a Drug Target for Individualized Therapy

Because *ZNF217* is overexpressed in poor prognostic and chemoresistant patients with breast cancer, we sought to identify drugs that kill tumor cells overexpressing *ZNF217*. We first used a candidate approach to determine whether AKT pathway inhibitors promoted cell death in a *ZNF217*-dependent manner, because *ZNF217* is required for and promotes AKT activation (Fig. 6C; ref. 23). MCF7 cells were infected with virus expressing short hairpin RNAs (shRNA) to *ZNF217* and validated for reduced protein expression (Supplementary Fig. S4E and S4F). Assaying cell death of MCF7 cells infected with lentivirus expressing scrambled or *ZNF217*-shRNA, we observed that the phosphoinositide 3-kinase (PI3K) inhibitor GDC0941 and the AKT inhibitor MK2206 did not induce *ZNF217*-dependent cell death (Fig. 6D).

We next used an *in silico* screening approach to identify candidate therapeutics that inhibit growth of cancer cells expressing high *ZNF217* at low drug concentrations. We determined *ZNF217* expression by qRT-PCR in the NCI60 panel of cell lines. We then used a drug data set from a panel of approximately 50,000 drugs generated by the NCI Developmental Therapeutics Program (<http://dtp.nci.nih.gov/>). Correlation of *ZNF217* expression in the cell line panel with the drug panel identified 15 drugs that selectively inhibited growth of cells

expressing high levels of *ZNF217*, as assessed by GI<sub>50</sub>, with a low drug concentration (Supplementary Table S5).

To determine whether *ZNF217* contributes to the drug-induced growth inhibition, we assayed cell death of MCF7 cells infected with lentivirus expressing stably integrated scrambled or *ZNF217*-shRNA knockdown constructs. As proof-of-concept, we tested bisacodyl, tricitiribine, nogalamycin, and 2E3E for their ability to influence cell death in culture in a *ZNF217*-dependent manner. Cells expressing reduced levels of *ZNF217* (*ZNF217*-shRNA) required higher concentrations of bisacodyl or tricitiribine for cell killing (Fig. 6E and F). Three different *ZNF217*-shRNA constructs gave similar results (Fig. 6 and data not shown). Nogalamycin or 2E2E treatment did not promote *ZNF217*-dependent cell death at a therapeutically possible concentration range (data not shown).

We focused on tricitiribine (also known as API-2), which is a nucleoside analogue and DNA synthesis inhibitor that has been tested in phase I clinical trials in patients with cancer as well as in one phase II clinical trial in patients with metastatic breast cancer (24–27). Cancer cells expressing high levels of *ZNF217* required lower concentrations of tricitiribine to inhibit growth than cells with low *ZNF217* expression (Fig. 6G and H). We then assayed tricitiribine on a panel of breast cancer cell lines that we previously analyzed for gene expression (28). The GI<sub>50</sub>s significantly correlated with *ZNF217* expression levels ( $r = -0.39$ ,  $P = 0.035$ ; Spearman; Fig. 6I), consistent with a selective effect of tricitiribine on cell lines that express the highest *ZNF217* levels.

### Tricitiribine Kills Cells *In Vivo* in Tumors That Overexpress *Znf217*

To test the effects of tricitiribine *in vivo*, we transplanted vector control and *Znf217*-overexpressing tumorigenic Vo-PyMT cells orthotopically to contralateral mammary fat pads cleared of epithelium. At 3 weeks, we injected mice with either tricitiribine or vehicle solution for 5 d/wk. Tricitiribine treatment significantly reduced to baseline levels the increase in tumor burden seen as a result of *Znf217* overexpression and led to reduced phospho-AKT expression, reduced phospho-MAPK expression, and increased cell death *in vivo* (Fig. 7A–C; Supplementary Fig. S4G). In culture, tricitiribine inhibited only phospho-AKT and did not inhibit phospho-MAPK or ErbB3 activation after heregulin stimulation (Fig. 7D). The observed differences between signaling events inhibited by tricitiribine in culture versus *in vivo* suggest that cells within a tumor microenvironment respond differently to tricitiribine than do cells in culture.

Tricitiribine also was effective *in vivo* at inhibiting tumor growth in mice xenografted with the human tumorigenic cell line MCF7 compared with control-treated mice (Fig. 7E).

### Tricitiribine Overcomes *ZNF217*-Induced Doxorubicin Resistance

Tumor cells overexpressing *ZNF217* are resistant to doxorubicin-induced cell death (23). Several groups have found tricitiribine to be an effective, synergistic therapy in combination with other drugs (e.g., trastuzumab, farnesyl-transferase inhibitors) to reduce tumor burden (29, 30). Similarly, we found that the addition of tricitiribine with doxorubicin to cells in culture generated a synthetic lethality in which cells overexpressing *ZNF217* were no longer resistant to doxorubicin and instead were killed (Fig. 7F). Interestingly, the parent mammary epithelial cell line HBL100 expresses low levels of adenosine kinase, which is required for the phosphorylation and activation of tricitiribine in patients. This suggests that *ZNF217* may be a sufficiently predictive biomarker of tricitiribine efficacy, even in patients with low adenosine kinase, if patients are also treated in combination with a drug such as doxorubicin.

## DISCUSSION

### ZNF217 Is a Biomarker of Disease Progression and Treatment Response and Is a Therapeutic Target Inhibited by Triciribine

In this study, we identified ZNF217 as a prognostic biomarker of reduced survival, metastasis, and chemoresistance in patients with breast cancer. Using both cultured cells and *in vivo* mouse transplant models, we found that *ZNF217* overexpression contributes to multiple aspects of carcinogenesis including increased proliferation/decreased cell death, increased invasiveness, increased motility, immortalization, chemotherapy resistance, metastasis, and progenitor cell expansion. Our data show that ZNF217 promotes carcinogenesis by driving a differentiation gene expression signature toward a less differentiated/progenitor state indicative of expanding a multipotent progenitor population.

We identified a panel of drugs that inhibit the growth of cell lines that overexpress *ZNF217* and validated two that induced ZNF217-dependent cell death.

### Triciribine: A Component of Therapy for Poor Prognostic Breast Cancer Patients

Triciribine is a nucleoside analogue and DNA synthesis inhibitor that has been tested in phase I clinical trials in patients with cancer as well as in one phase II clinical trial in patients with metastatic breast cancer (24–27). In the phase II study, one of 14 patients had stable disease and the other patients progressed (27). The phase II studies and subsequent studies found that triciribine was not readily bioactive in all patients, possibly due to the requirement for expression of multiple genes for triciribine bioactivation. Triciribine is also an allosteric inhibitor of AKT activation: it physically interacts with AKT to prevent AKT recruitment to the plasma membrane and to block the phosphorylation and activation of AKT (31, 32).

Although several studies identified triciribine as an AKT inhibitor, triciribine is not always redundant with other AKT pathway inhibitors in treating tumors: often triciribine is more effective *in vivo* than other PI3K/AKT pathway inhibitors at inhibiting tumor progression (29). Indeed, we found that triciribine inhibited not only AKT activation but also MAPK activation *in vivo* (Fig. 7B and C). We hypothesize that triciribine inhibits both AKT and MAPK pathways, both of which are downstream of ERBB3/ERBB2 activation. This could provide a rationale for inhibition of ZNF217-induced tumor burden by triciribine because ZNF217 drives the over-expression of ERBB3 and leads to the activation of both AKT and MAPK pathways. Alternatively, triciribine could inhibit these pathways after activation of other receptor tyrosine kinases (Fig. 7G).

Our study suggests that ZNF217 may be a sufficiently predictive biomarker of triciribine efficacy if patients are also treated in combination with a drug such as doxorubicin or another drug that offers synergy with triciribine. In part, ZNF217 may act by inducing upregulation of its target ERBB3 (22). Thus, cells resistant to triciribine treatment might independently activate multiple signaling pathways, making them less responsive to inhibitors that act upstream in the signaling pathway.

Combinatorial pathway activation may be therapeutically important in treating patients with high *ZNF217* expression, as concurrent activation of the PI3K/AKT and RAS/MAPK pathways causes resistance to AKT inhibition in cells (33). Interestingly, in the panel of immortal cell lines expressing *ZNF217* and tested for triciribine sensitivity, all outlier cell lines (i.e., lines with high GI<sub>50</sub>s and high *ZNF217* expression) contained previously identified mutations in the PI3K/AKT and/or RAS/MAPK pathways (34–36). Because triciribine does not inhibit upstream activators PI3K or PDK1 or related family members directly (31), future studies will be required to sort out mechanistically how ZNF217

activates and triciribine inhibits signaling. Whether combination therapies will be more effective *in vivo* remains to be tested.

### ZNF217 Reprograms Tumor Cells to Express Luminal and Myoepithelial Cell Markers

We found that ZNF217 promotes phenotypes suggestive of expansion of progenitor cells *in vivo* and in culture and drives repression of an adult stem cell gene expression signature that is also downregulated in many epithelial cancers. Consistent with a progenitor phenotype, ZNF217 promotes increased telomerase, resistance to TGF $\beta$  growth inhibition, amplified *c-MYC* (9, 37), and chemotherapy resistance (23). That ZNF217 may drive a less differentiated gene expression signature is supported by the observation that *Znf217* is upregulated in the somite following the transition from the presomitic mesoderm and before the differentiation into the skeleton, muscle, and dermis (38). Moreover, *Znf217* is repressed concurrently with *Oct4* following differentiation of a teratocarcinoma cell line to neuronal cells and binds to the promoters of a number of genes involved in differentiation (10). Thus, in tumors, ZNF217 may promote transdifferentiation to or expansion of a pool of progenitor-like cells by aberrantly suppressing differentiation pathways.

*Znf217* overexpression in tumor cells derived from mice expressing the oncogene PyMT switched their phenotype from a predominantly luminal to a more heterogeneous pathology characterized by expression of both luminal and myoepithelial cell markers. This phenotype is similar to that seen following *Wnt1* overexpression or activation of the AKT pathway by PTEN deletion *in vivo* (39, 40). Interestingly, the PyMT oncogene can give rise to tumors expressing both luminal and myoepithelial markers, depending on the cell type into which it is introduced. Expression of PyMT by intraductal injection of avian retrovirus (RCAS-PyMT) induces tumors with markers of luminal, myoepithelial, and progenitor cells (41). Recently, a connection has emerged between the undifferentiated, stem cell-like phenotype in breast cancer cells and transdifferentiation of the tumor cells toward a mesenchymal phenotype (reviewed in refs. 42–44). Induction of EMT in cultured MECs not only increases the population of cells with mesenchymal markers but also increases those with progenitor cell characteristics (CD44<sup>high</sup>/CD24<sup>low</sup>; ref. 45).

## CONCLUSIONS

We used an integrated biologic approach to model the multiple contributions of ZNF217 to carcinogenesis during tumor progression, metastasis, and neoadjuvant treatment. We propose that ZNF217 is a biomarker that is prognostic of disease progression and is a therapeutic target. Our data suggest that triciribine may be a component of an effective treatment strategy in patients who have tumors expressing high ZNF217, possibly by targeting a progenitor population and reducing signaling in the AKT and MAPK pathways. Because *ZNF217* is amplified in numerous cancers, this work has implications for other cancers as well.

## METHODS

Additional descriptions of materials and methods, including cell lines, antibodies, and staining procedures used, are in the Supplementary Data.

### Cell Lines

Cell lines used in this study include mouse MECs NMuMG (source: Rik Derynck), SCp2 (source: Mina Bissell), EpH4 (source: Mina Bissell), and Vo-PyMT-Luc (source: Conor Lynch) and human MEC lines MCF7, ZR-75-1, and HBL100 (source: American Type

Culture Collection for all 3 lines). MCF7 was authenticated by SNP6.0 copy number analysis. Other cell lines were not authenticated.

### Mouse Lines

Mice used in this study were maintained on the FVB/n background under pathogen-free conditions in the University of California, San Francisco (San Francisco, CA; UCSF) barrier facility. Our animal protocols were reviewed and approved by the UCSF Institution Animal Care and Use Committee.

### Metastasis Analysis

Both PyMT MEC and Vo-PyMT transplants were analyzed for lung metastasis. To determine metastasis frequency, lung tissue blocks were sectioned into 5- $\mu$ m sections and stained by hematoxylin and eosin. For each mouse analyzed, one section was scored for number of metastases seen at  $\times 100$  magnification in 3 (PyMT MECs) or 5 (Vo-PyMT cell line) high-powered fields in regions of the tissue section with the highest density of metastases. Each cohort had 6 to 11 mice analyzed.

### Statistical Analysis

Statistical analysis was conducted using Prism 4 software (Graph-Pad Software, Inc.) or SPSS Statistics software (IBM) for Cox proportional hazard tests. Cohorts of 3 or more samples were compared using one-way ANOVA. All tests used and *P* values are specified in the figure legends. *P* < 0.05 was considered significant.

### Accession Numbers

Microarray data were deposited to the NCBI's GEO Repository and are accessible to readers through GEO series accession number GSE24727.

### Supplementary Material

Refer to Web version on PubMed Central for supplementary material.

### Acknowledgments

The authors thank members of the Werb laboratory, Lewis Cantley, and Gordon Mills for helpful discussions throughout this project; Ying Yu for genotyping; Elena Atamaniuc for tumor measurements, and Jimmy Hwang for statistical advice.

#### Grant Support

This work was supported by grants from the NIH (CA129523 and CA129523-02S1 to Z. Werb, CA058207 to J.W. Gray and Z. Werb, and ES019458 to Z. Werb and P. Yaswen), a Stand Up To Cancer Dream Team Translational Cancer Research Grant, a Program of the Entertainment Industry Foundation [SU2C-AACR-DT0409 (to Z. Werb and J.W. Gray)], an American Cancer Society Postdoctoral fellowship and a Ruth L. Kirschstein National Research Service award CA103534 (to L.E. Littlepage), a Canadian Institutes of Health Research Postdoctoral fellowship (to O.L. Griffith), and a Career Development Award from Bay Area Breast Specialized Programs of Research Excellence CA058207 (to M.D. Sternlicht).

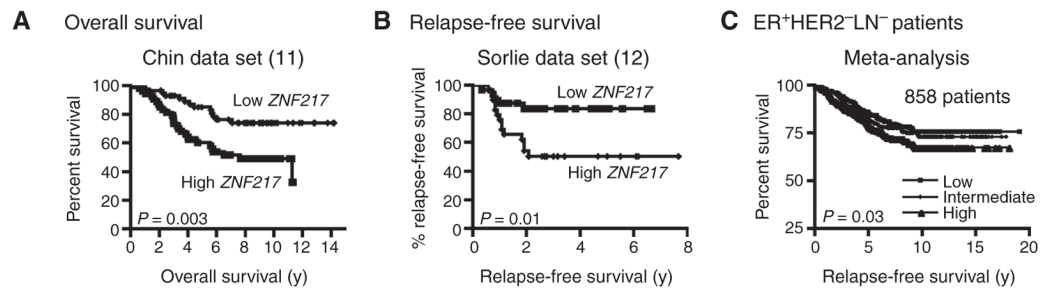
### References

1. Collins C, Rommens JM, Kowbel D, Godfrey T, Tanner M, Hwang SI, et al. Positional cloning of ZNF217 and NABC1: genes amplified at 20q13. 2 and overexpressed in breast carcinoma. *Proc Natl Acad Sci U S A*. 1998; 95:8703–8. [PubMed: 9671742]

2. Collins C, Volik S, Kowbel D, Ginzinger D, Ylstra B, Cloutier T, et al. Comprehensive genome sequence analysis of a breast cancer amplicon. *Genome Res.* 2001; 11:1034–42. [PubMed: 11381030]
3. You A, Tong JK, Grozinger CM, Schreiber SL. CoREST is an integral component of the CoREST-human histone deacetylase complex. *Proc Natl Acad Sci U S A.* 2001; 98:1454–8. [PubMed: 11171972]
4. Shi Y, Sawada J, Sui G, Affar el B, Whetstine JR, Lan F, et al. Coordinated histone modifications mediated by a CtBP co-repressor complex. *Nature.* 2003; 422:735–8. [PubMed: 12700765]
5. Quinlan KG, Nardini M, Verger A, Francescato P, Yaswen P, Corda D, et al. Specific recognition of ZNF217 and other zinc finger proteins at a surface groove of C-terminal binding proteins. *Mol Cell Biol.* 2006; 26:8159–72. [PubMed: 16940172]
6. Cowger JJ, Zhao Q, Isovich M, Torchia J. Biochemical characterization of the zinc-finger protein 217 transcriptional repressor complex: identification of a ZNF217 consensus recognition sequence. *Oncogene.* 2007; 26:3378–86. [PubMed: 17130829]
7. Thillainadesan G, Isovich M, Loney E, Andrews J, Tini M, Torchia J. Genome analysis identifies the p15ink4b tumor suppressor as a direct target of the ZNF217/CoREST complex. *Mol Cell Biol.* 2008; 28:6066–77. [PubMed: 18625718]
8. Banck MS, Li S, Nishio H, Wang C, Beutler AS, Walsh MJ. The ZNF217 oncogene is a candidate organizer of repressive histone modifiers. *Epigenetics.* 2009; 4:100–6. [PubMed: 19242095]
9. Nonet GH, Stampfer MR, Chin K, Gray JW, Collins CC, Yaswen P. The ZNF217 gene amplified in breast cancers promotes immortalization of human mammary epithelial cells. *Cancer Res.* 2001; 61:1250–4. [PubMed: 11245413]
10. Krig SR, Jin VX, Bieda MC, O'Geen H, Yaswen P, Green R, et al. Identification of genes directly regulated by the oncogene ZNF217 using chromatin immunoprecipitation (ChIP)-chip assays. *J Biol Chem.* 2007; 282:9703–12. [PubMed: 17259635]
11. Chin K, DeVries S, Fridlyand J, Spellman PT, Roydasgupta R, Kuo WL, et al. Genomic and transcriptional aberrations linked to breast cancer pathophysiologies. *Cancer Cell.* 2006; 10:529–41. [PubMed: 17157792]
12. Sorlie T, Perou CM, Fan C, Geisler S, Aas T, Nobel A, et al. Gene expression profiles do not consistently predict the clinical treatment response in locally advanced breast cancer. *Mol Cancer Ther.* 2006; 5:2914–8. [PubMed: 17121939]
13. Wong DJ, Liu H, Ridky TW, Cassarino D, Segal E, Chang HY. Module map of stem cell genes guides creation of epithelial cancer stem cells. *Cell Stem Cell.* 2008; 2:333–44. [PubMed: 18397753]
14. Woodward WA, Chen MS, Behbod F, Rosen JM. On mammary stem cells. *J Cell Sci.* 2005; 118:3585–94. [PubMed: 16105882]
15. Wang XY, Yin Y, Yuan H, Sakamaki T, Okano H, Glazer RI. Musashi1 modulates mammary progenitor cell expansion through proliferin-mediated activation of the Wnt and Notch pathways. *Mol Cell Biol.* 2008; 28:3589–99. [PubMed: 18362162]
16. Villadsen R, Fridriksdottir AJ, Ronnov-Jessen L, Gudjonsson T, Rank F, LaBarge MA, et al. Evidence for a stem cell hierarchy in the adult human breast. *J Cell Biol.* 2007; 177:87–101. [PubMed: 17420292]
17. McCaffrey LM, Macara IG. The Par3/aPKC interaction is essential for end bud remodeling and progenitor differentiation during mammary gland morphogenesis. *Genes Dev.* 2009; 23:1450–60. [PubMed: 19528321]
18. Gudjonsson T, Villadsen R, Nielsen HL, Ronnov-Jessen L, Bissell MJ, Petersen OW. Isolation, immortalization, and characterization of a human breast epithelial cell line with stem cell properties. *Genes Dev.* 2002; 16:693–706. [PubMed: 11914275]
19. Minn AJ, Gupta GP, Siegel PM, Bos PD, Shu W, Giri DD, et al. Genes that mediate breast cancer metastasis to lung. *Nature.* 2005; 436:518–24. [PubMed: 16049480]
20. Li X, Lewis MT, Huang J, Gutierrez C, Osborne CK, Wu MF, et al. Intrinsic resistance of tumorigenic breast cancer cells to chemotherapy. *J Natl Cancer Inst.* 2008; 100:672–9. [PubMed: 18445819]

21. Hess KR, Anderson K, Symmans WF, Valero V, Ibrahim N, Mejia JA, et al. Pharmacogenomic predictor of sensitivity to preoperative chemotherapy with paclitaxel and fluorouracil, doxorubicin, and cyclophosphamide in breast cancer. *J Clin Oncol*. 2006; 24:4236–44. [PubMed: 16896004]
22. Krig SR, Miller JK, Fritze S, Beckett LA, Neve RM, Farnham PJ, et al. ZNF217, a candidate breast cancer oncogene amplified at 20q13, regulates expression of the ErbB3 receptor tyrosine kinase in breast cancer cells. *Oncogene*. 2010; 29:5500–10. [PubMed: 20661224]
23. Huang G, Krig S, Kowbel D, Xu H, Hyun B, Volik S, et al. ZNF217 suppresses cell death associated with chemotherapy and telomere dysfunction. *Hum Mol Genet*. 2005; 14:3219–25. [PubMed: 16203743]
24. Schilcher RB, Haas CD, Samson MK, Young JD, Baker LH. Phase I evaluation and clinical pharmacology of tricyclic nucleoside 5'-phosphate using a weekly intravenous regimen. *Cancer Res*. 1986; 46:3147–51. [PubMed: 3698029]
25. Feun LG, Savaraj N, Bodey GP, Lu K, Yap BS, Ajani JA, et al. Phase I study of tricyclic nucleoside phosphate using a five-day continuous infusion schedule. *Cancer Res*. 1984; 44:3608–12. [PubMed: 6744283]
26. Garrett CR, Coppola D, Wenham RM, Cubitt CL, Neuger AM, Frost TJ, et al. Phase I pharmacokinetic and pharmacodynamic study of triciribine phosphate monohydrate, a small-molecule inhibitor of AKT phosphorylation, in adult subjects with solid tumors containing activated AKT. *Invest New Drugs*. 2011; 29:1381–9. [PubMed: 20644979]
27. Hoffman K, Holmes FA, Fraschini G, Esparza L, Frye D, Raber MN, et al. Phase I-II study: triciribine (tricyclic nucleoside phosphate) for metastatic breast cancer. *Cancer Chemother Pharmacol*. 1996; 37:254–8. [PubMed: 8529286]
28. Neve RM, Chin K, Fridlyand J, Yeh J, Baehner FL, Fevr T, et al. A collection of breast cancer cell lines for the study of functionally distinct cancer subtypes. *Cancer Cell*. 2006; 10:515–27. [PubMed: 17157791]
29. Lu CH, Wyszomierski SL, Tseng LM, Sun MH, Lan KH, Neal CL, et al. Preclinical testing of clinically applicable strategies for overcoming trastuzumab resistance caused by PTEN deficiency. *Clin Cancer Res*. 2007; 13:5883–8. [PubMed: 17908983]
30. Balasis ME, Forinash KD, Chen YA, Fulp WJ, Coppola D, Hamilton AD, et al. Combination of farnesyltransferase and Akt inhibitors is synergistic in breast cancer cells and causes significant breast tumor regression in ErbB2 transgenic mice. *Clin Cancer Res*. 2011; 17:2852–62. [PubMed: 21536547]
31. Yang L, Dan HC, Sun M, Liu Q, Sun XM, Feldman RI, et al. Akt/protein kinase B signaling inhibitor-2, a selective small molecule inhibitor of Akt signaling with antitumor activity in cancer cells overexpressing Akt. *Cancer Res*. 2004; 64:4394–9. [PubMed: 15231645]
32. Berndt N, Yang H, Trinczek B, Betzi S, Zhang Z, Wu B, et al. The Akt activation inhibitor TCN-P inhibits Akt phosphorylation by binding to the PH domain of Akt and blocking its recruitment to the plasma membrane. *Cell Death Differ*. 2010; 17:1795–804. [PubMed: 20489726]
33. She QB, Halilovic E, Ye Q, Zhen W, Shirasawa S, Sasazuki T, et al. 4E-BP1 is a key effector of the oncogenic activation of the AKT and ERK signaling pathways that integrates their function in tumors. *Cancer Cell*. 2010; 18:39–51. [PubMed: 20609351]
34. Hoeflich KP, O'Brien C, Boyd Z, Cavet G, Guerrero S, Jung K, et al. *In vivo* antitumor activity of MEK and phosphatidylinositol 3-kinase inhibitors in basal-like breast cancer models. *Clin Cancer Res*. 2009; 15:4649–64. [PubMed: 19567590]
35. Hollestelle A, Nagel JH, Smid M, Lam S, Elstrodt F, Wasielewski M, et al. Distinct gene mutation profiles among luminal-type and basal-type breast cancer cell lines. *Breast Cancer Res Treat*. 2010; 121:53–64. [PubMed: 19593635]
36. She QB, Chandralapaty S, Ye Q, Lobo J, Haskell KM, Leander KR, et al. Breast tumor cells with PI3K mutation or HER2 amplification are selectively addicted to Akt signaling. *PLoS One*. 2008; 3:e3065. [PubMed: 18725974]
37. Li P, Maines-Bandiera S, Kuo WL, Guan Y, Sun Y, Hills M, et al. Multiple roles of the candidate oncogene ZNF217 in ovarian epithelial neoplastic progression. *Int J Cancer*. 2007; 120:1863–73. [PubMed: 17266044]

38. Buttitta L, Tanaka TS, Chen AE, Ko MS, Fan CM. Microarray analysis of somitogenesis reveals novel targets of different WNT signaling pathways in the somitic mesoderm. *Dev Biol.* 2003; 258:91–104. [PubMed: 12781685]
39. Li Y, Welm B, Podsypanina K, Huang S, Chamorro M, Zhang X, et al. Evidence that transgenes encoding components of the Wnt signaling pathway preferentially induce mammary cancers from progenitor cells. *Proc Natl Acad Sci U S A.* 2003; 100:15853–8. [PubMed: 14668450]
40. Korkaya H, Paulson A, Charafe-Jauffret E, Ginestier C, Brown M, Dutcher J, et al. Regulation of mammary stem/progenitor cells by PTEN/Akt/beta-catenin signaling. *PLoS Biol.* 2009; 7:e1000121. [PubMed: 19492080]
41. Du Z, Podsypanina K, Huang S, McGrath A, Toneff MJ, Bogoslovskaja E, et al. Introduction of oncogenes into mammary glands *in vivo* with an avian retroviral vector initiates and promotes carcinogenesis in mouse models. *Proc Natl Acad Sci U S A.* 2006; 103:17396–401. [PubMed: 17090666]
42. Blick T, Hugo H, Widodo E, Waltham M, Pinto C, Mani SA, et al. Epithelial mesenchymal transition traits in human breast cancer cell lines parallel the CD44(hi)/CD24 (lo/-) stem cell phenotype in human breast cancer. *J Mammary Gland Biol Neoplasia.* 2010; 15:235–52. [PubMed: 20521089]
43. Polyak K, Weinberg RA. Transitions between epithelial and mesenchymal states: acquisition of malignant and stem cell traits. *Nat Rev Cancer.* 2009; 9:265–73. [PubMed: 19262571]
44. Thiery JP, Acloque H, Huang RY, Nieto MA. Epithelial-mesenchymal transitions in development and disease. *Cell.* 2009; 139:871–90. [PubMed: 19945376]
45. Mani SA, Guo W, Liao MJ, Eaton EN, Ayyanan A, Zhou AY, et al. The epithelial-mesenchymal transition generates cells with properties of stem cells. *Cell.* 2008; 133:704–15. [PubMed: 18485877]

**Figure 1.**

*ZNF217* overexpression is a prognostic indicator in patients with breast cancer. **A**, patients ( $N = 118$ ; ref. 11) were separated by high ( $n = 59$ ) versus low ( $n = 59$ ) *ZNF217* expression and analyzed for overall survival ( $P = 0.003$ ; log-rank). **B**, relapse-free survival (12) based on high ( $n = 40$ ) versus low ( $n = 41$ ) *ZNF217* expression ( $P = 0.01$ ; log-rank). **C**, patients ( $N = 858$ ) were separated by low ( $n = 286$ ), intermediate ( $n = 286$ ), and high ( $n = 286$ ) *ZNF217* expression and analyzed for relapse-free survival. Patients with high *ZNF217* expression had worse survival than low *ZNF217* patients ( $P = 0.03$ ; log-rank) as described in Supplementary Materials.

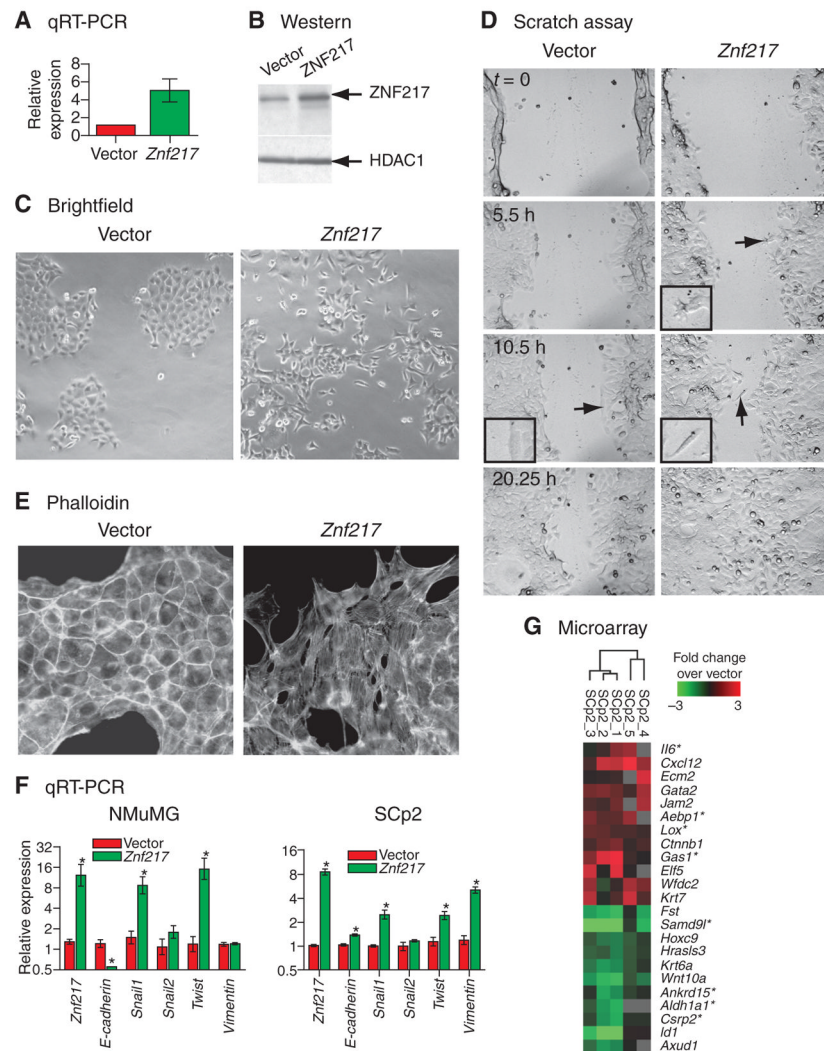


**Figure 2.** *Znf217* overexpression promotes increased cell motility and aberrant epithelial marker expression. **A**, relative *Znf217* expression levels by qRT-PCR in SCp2 mammary epithelial cell lines infected with virus to overexpress vector or *Znf217* with comparable results in 3 experiments. Each sample was tested by qRT-PCR in triplicate relative to the reference *TATA box binding protein (Tbp)*, with similar results for other reference genes. Graphs show the mean  $\pm$  SEM. **B**, Western blot analysis of ZNF217 protein (anti-ZNF217) and loading control (anti-HDAC1) in SCp2 cells. Images are representative of multiple experiments using retrovirus or lentivirus overexpression of *Znf217*. Arrows mark the indicated proteins. **C**, brightfield images of SCp2 cells  $\pm$  *Znf217* display increased cell scattering in culture after *Znf217* overexpression. **D**, frames from movies of SCp2 cells infected with vector or ZNF217 following a scratch with a pipette tip. The movies ran 20.25 hours. Note the lamellipodia (arrow) extending from the cells by 5.5 hours and the increased number of *Znf217*-expressing cells in the middle of the scratch by 10.5 hours (arrow). **E**, phalloidin staining of SCp2 cells *Znf217*. **F**, relative expression of *Znf217* and selected genes by qRT-PCR from NMuMG (top) and SCp2 (bottom) cells  $\pm$  *Znf217* *in vitro*. Graph shows the mean  $\pm$  SEM, relative to the reference *Gapdh*. Similar results were seen with the reference *Hprt*. For each gene, samples for *Znf217* were compared with vector by Mann–

Whitney tests, and significant *P* values <0.02 were marked with \*. **G**, heat map of selected genes enriched following *Znf217* overexpression in SCp2 cells. *Gapdh*, glyceraldehyde-3-phosphate dehydrogenase; *Hprt*, hypoxanthine phosphoribosyltransferase.

\$watermark-text

\$watermark-text

\$watermark-text

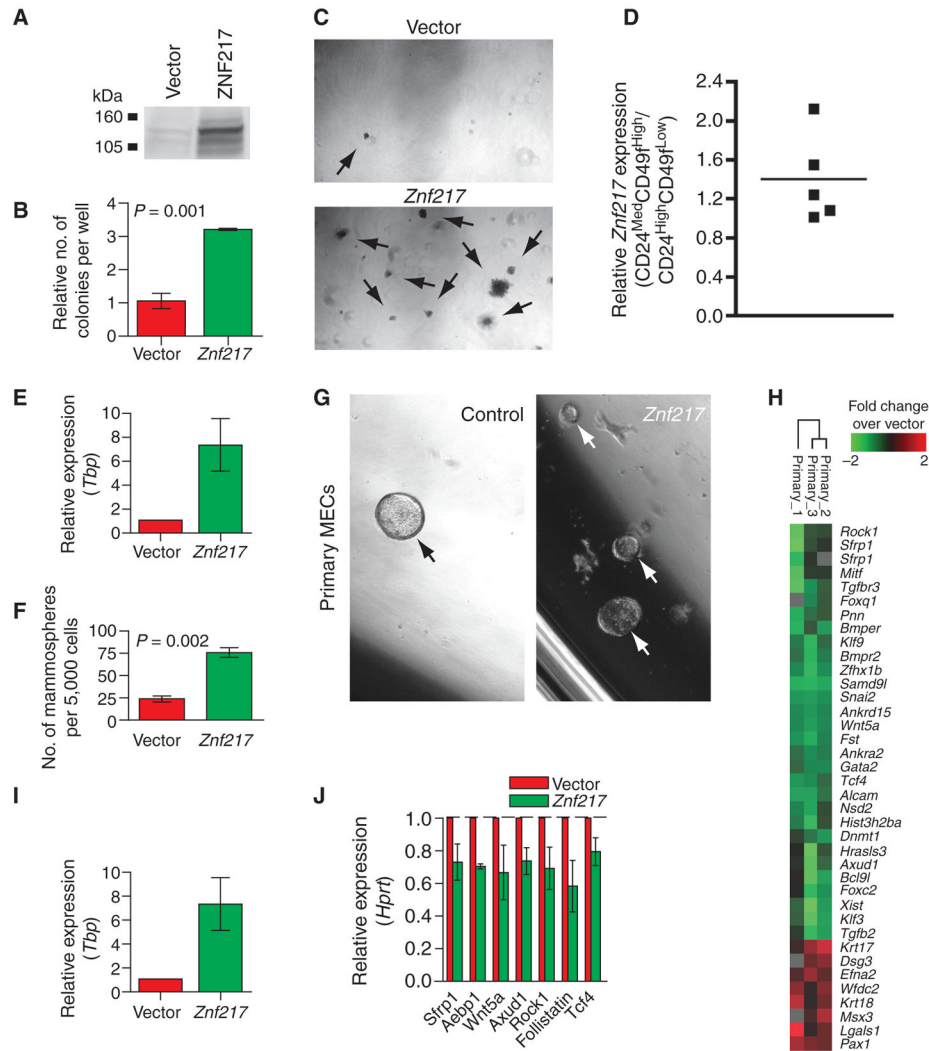


**Figure 3.** *Znf217* overexpression causes an increase in soft agar colonies and in mammosphere formation. **A**, Western blot analysis of ZNF217 protein in NIH3T3 cells infected with vector or *Znf217* retrovirus. **B**, *Znf217* overexpression increases the number of colonies by anchorage-independent growth in soft agar assay. Relative number of colonies per well by soft agar with vector or *Znf217* overexpression ( $P = 0.001$ ; Student *t* test). Graph compiles results from 3 experiments, each done in triplicate. **C**, brightfield images of anchorage-independent colonies from soft agar assay  $\pm$  ZNF217 in **B**. Arrows mark examples of colonies. The large colonies were only seen with the *Znf217*-overexpressing cells, whereas much smaller colonies were seen with vector-expressing cells. **D**, relative expression of *Znf217* by qRT-PCR from normal adult mammary gland (FVB/n), relative to the reference *Hprt* with line marking the mean. Glands were sorted by flow cytometry for CD24<sup>Med</sup>CD49f<sup>High</sup> (basal/myoepithelial/progenitor cells) and CD24<sup>High</sup>CD49f<sup>Low</sup> (luminal/luminal progenitor) fractions. RNA was isolated and used to generate cDNA from each population. Each dot represents one mouse sorted, collected, and processed by qRT-PCR. Graph shows relative epithelial *Znf217* expression in the CD24<sup>Med</sup>CD49f<sup>High</sup> versus CD24<sup>High</sup>CD49f<sup>Low</sup> populations. Similar results were seen with the reference *Gapdh*. **E**, relative expression of *Znf217* by qRT-PCR in primary mouse MECs following lenti-viral

infection with either pEiT vector or *Znf217*-pEiT in 3 separate samples. Each sample was tested by qRT-PCR in triplicate relative to the reference *Tbp*. These samples were used for microarray analysis. Graph shows the mean  $\pm$  SEM. Quantification (**F**) and brightfield images (**G**) of mammosphere assay of Vo-PyMT cells overexpressing vector or *Znf217*. **H**, heat map of selected genes from gene expression microarray analysis enriched in primary MECs overexpressing *Znf217*. **I**, relative expression of *Znf217* by qRT-PCR in primary mouse MECs following lentiviral infection with either vector or *Znf217* in 3 separate samples. Each sample was tested by qRT-PCR in triplicate relative to the reference *Tbp* and used for microarray analysis. Graph shows the mean  $\pm$  SEM. **J**, qRT-PCR to validate microarray targets using the same samples used in (**H**) with *Hprt* as a reference in qRT-PCR reactions. Similar results were obtained with *Gapdh* used as a reference (data not shown). *Gapdh*, glyceraldehyde-3-phosphate dehydrogenase; *Hprt*, hypoxanthine phosphoribosyltransferase.

\$watermark-text

\$watermark-text

\$watermark-text

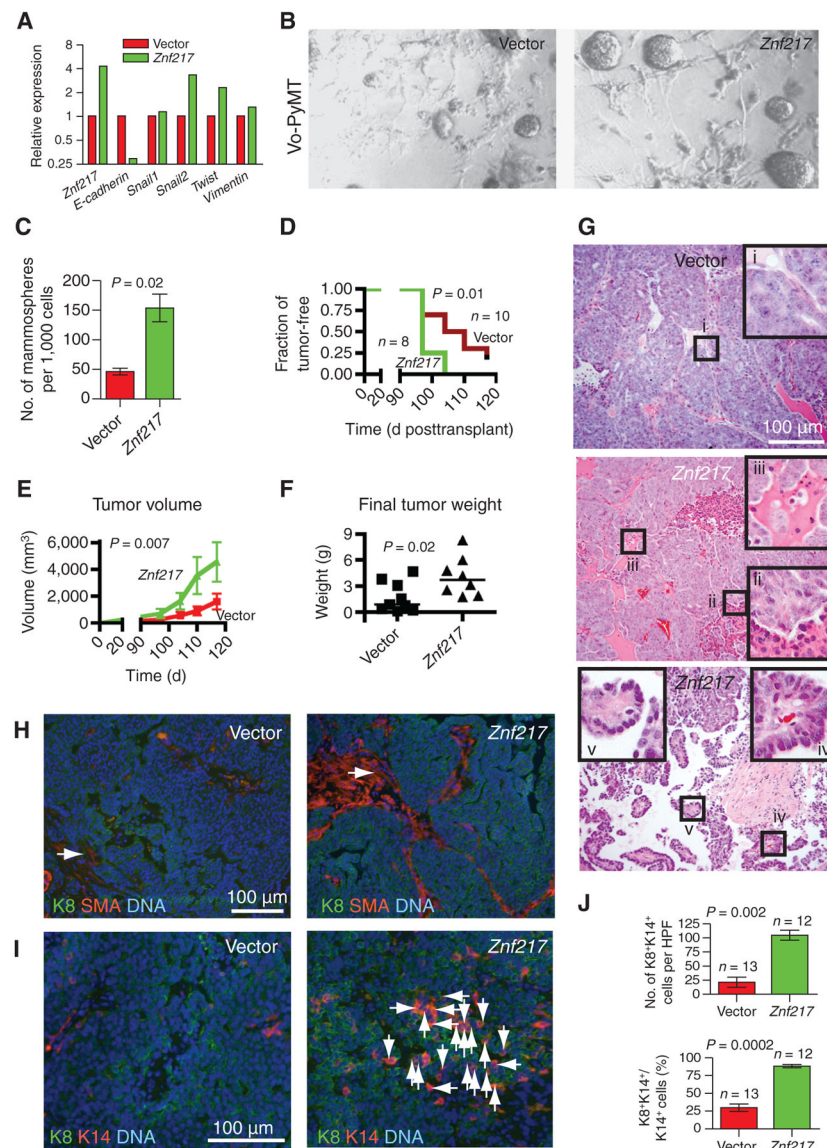


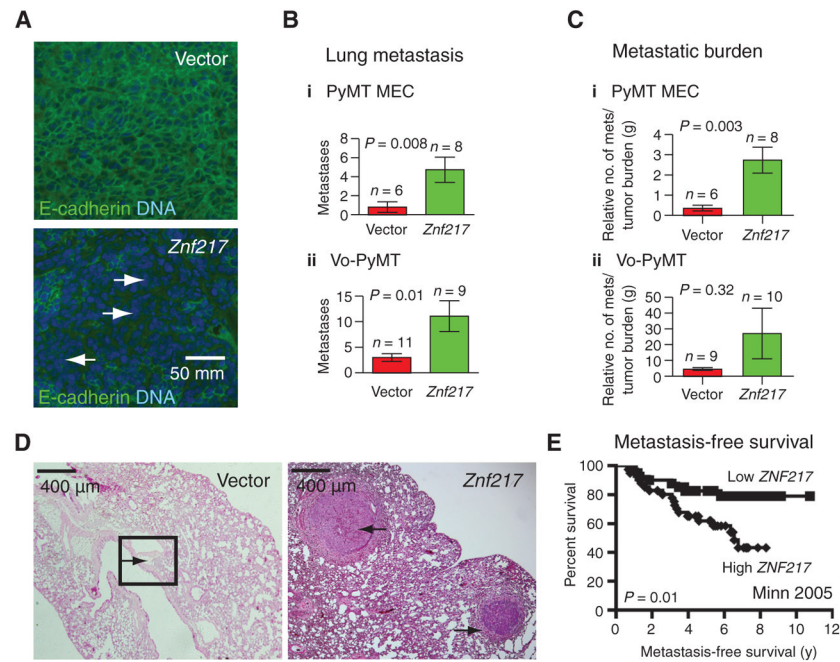
**Figure 4.** *Znf217* overexpression *in vivo* increases rate of tumor progression, tumor heterogeneity, and differentiation state. **A**, relative expression of *Znf217* and *EMT* genes by qRT-PCR in the Vo-PyMT cell line overexpressing either vector or *Znf217*. The assay used the reference *Gapdh*. Similar results were seen using *Hprt* or *Tbp* references. The cells used in this experiment had previously been sorted for fluorescent marker expression and were used for the Vo-PyMT transplants throughout this study. **B**, mammosphere assay of primary MECs infected with vector or *Znf217*-overexpressing lentivirus. **C**, quantification of mammosphere formation in primary MECs expressing vector or *Znf217* after 1 week. Graph shows mean  $\pm$  SEM, and samples were compared by unpaired *t* test. **D**, tumor-free survival over time in Vo-PyMT transplants ( $P = 0.01$ ; log-rank). **E**, tumor volume over time in Vo-PyMT transplants of *Znf217* ( $n = 8$ ) versus vector ( $n = 10$ ;  $P = 0.007$ ; ANOVA, repeated measures). **F**, final tumor weight in Vo-PyMT transplants ( $P = 0.02$ ; Mann-Whitney). Line represents median of vector ( $n = 9$ ) versus *Znf217* ( $n = 8$ ). **G**, H&E staining of MMTV-PyMT (PyMT MEC) tumors from transplants overexpressing vector (top) or *Znf217*

(middle, bottom). Insets are enlarged images of boxed regions and show heterogeneous pathology. **H**, immunofluorescence staining with anti-Keratin-8 (green), anti- $\alpha$ -SMA (red; arrows), and DNA (Hoechst; blue) in tumors derived from PyMT MEC transplants. **I**, immunofluorescence staining with anti-Keratin-8 (green), keratin-14 (red), and DNA (blue) from PyMT MEC transplants. Arrows mark cells double-positive for K8 and K14. **J**, quantification of a progenitor cell population: K8<sup>+</sup>K14<sup>+</sup> ( $P=0.002$ ), percentage of K8<sup>+</sup>K14<sup>+</sup> ( $P=0.0002$ ; unpaired  $t$  tests). Bar graphs show mean representation [ $n$  (%)] of K8<sup>+</sup>K14<sup>+</sup> cells  $\pm$  SEM per HPF. *Gapdh*, glyceraldehyde-3-phosphate dehydrogenase; HPF, 3 high-powered fields. *Hprt*, hypoxanthine phosphoribosyltransferase.

\$watermark-text

\$watermark-text

\$watermark-text

**Figure 5.**

*Znf217* overexpression *in vivo* increases lung metastasis. **A**, immunofluorescence with anti-E-cadherin (green) and DNA (blue) from Vo-PyMT transplants. Arrows mark regions with low E-cadherin expression. **B**, number of lung metastases per 3 (i) or 5 (ii) high-powered fields from (i) PyMT MEC ( $P = 0.008$ ) or (ii) Vo-PyMT transplants ( $P = 0.01$ ; Mann–Whitney) with vector or *Znf217* overexpression. Bar graph shows the mean  $\pm$  SEM. **C**, metastatic burden from PyMT and Vo-PyMT transplants. Number of lung metastases per 3 (PyMT) or 5 (Vo-PyMT) high-powered fields divided by tumor weight from (i) PyMT MEC ( $P = 0.003$ ; Mann–Whitney) or (ii) Vo-PyMT ( $P = 0.32$ ; Mann–Whitney) transplants with vector or *Znf217* overexpression. Bar graph shows the mean  $\pm$  SEM. Similar results were obtained using final tumor volume (data not shown). **D**, H&E staining of lung metastases from PyMT MEC transplants. Arrows mark examples of metastases. **E**, metastasis-free survival based on high ( $n = 41$ ) versus low ( $n = 41$ ) *ZNF217* expression ( $P = 0.01$ ; log-rank) from the work of Minn and colleagues (19).

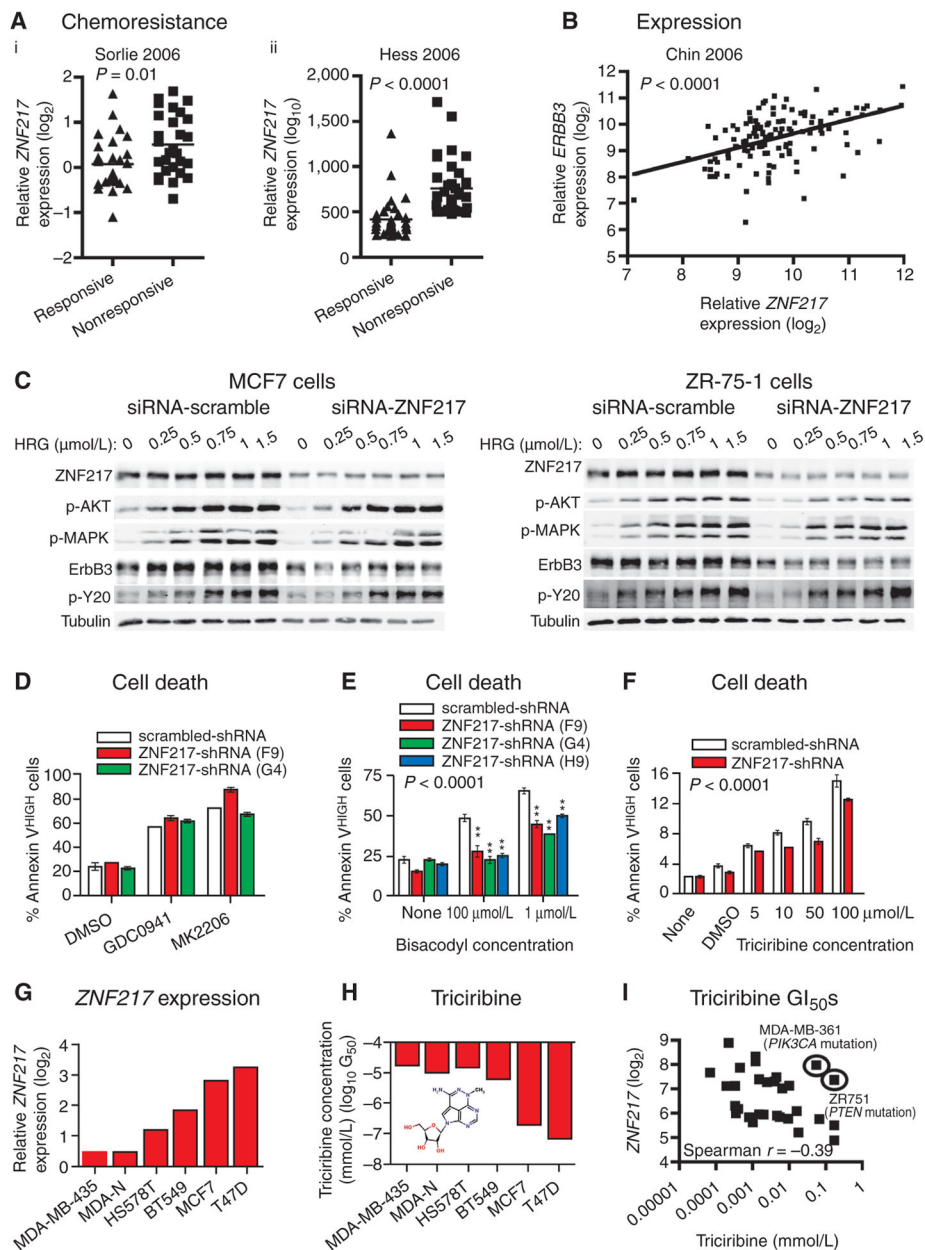


**Figure 6.** Identification of triciribine as a candidate inhibitor of ZNF217-induced growth. **A**, response to neoadjuvant chemotherapy in patients with breast cancer with high versus low *ZNF217* expression in tumors (i) from the work of Sorlie and colleagues (12). Patients had responsive ( $n = 27$ ) or non-responsive (stable/progressive) disease ( $n = 28$ ) in response to treatment ( $P = 0.01$ ; Mann–Whitney). Lines mark means; (ii) from Hess and colleagues (ref. 21;  $P < 0.001$ ; Mann–Whitney). Tumors were responsive (pathologic complete response;  $n = 34$ ) or nonresponsive (residual disease;  $n = 34$ ) to treatment. Lines mark means. **B**, *ZNF217* and *ERBB3* expression levels in human breast tumors ( $n = 118$ ) from Chin and colleagues (11). *ZNF217* and *ERBB3* strongly correlate (Pearson  $r = 0.47$ ;  $R^2 = 0.22$ ; by linear regression,  $P < 0.0001$ ). **C**, MCF7 cells (left) or ZR-75-1 cells (right) were transiently transfected with scrambled or ZNF217-siRNA. Forty-eight hours after transfection, cells were serum-starved

24 hours and treated for 15 minutes with heregulin. Lysates were blotted for the indicated proteins. **D**, PI3K and AKT inhibitors do not promote ZNF217-dependent cell death. Fluorescence-activated cell-sorting (FACS) analysis of cell death by Annexin V staining in MCF7 cells  $\pm$  ZNF217-shRNA or scramble control and treated for 2 days with control, 2  $\mu$ mol/L GDC0941, or 10  $\mu$ mol/L MK2206. **E**, treatment of MCF7 cells  $\pm$  ZNF217-shRNA with bisacodyl in triplicate at the indicated concentrations ( $P = 0.001$ ; ANOVA). Similar results were obtained in at least 3 experiments. **F**, treatment of MCF7 cells  $\pm$  ZNF217-shRNA with 10  $\mu$ mol/L triciribine at the indicated concentrations ( $P = 0.001$ ; ANOVA). Similar results were obtained with a second shRNA and in at least 3 experiments. **ZNF217** (**G**) expression levels and related triciribine GI<sub>50</sub> concentrations (**H**) in NCI60 panel breast cancer cell lines. Inset, chemical structure of triciribine. **I**, ZNF217 expression levels (Neve data set, ref. 28) across triciribine GI<sub>50</sub>s in 30 breast cancer cell lines (15 each of cell lines expressing highest/lowest ZNF217;  $r = -0.39$ ;  $P = 0.035$ ; Spearman correlation). Two outliers circled are identified by cell type and relevant mutations. DMSO, dimethyl sulfoxide.

\$watermark-text

\$watermark-text

\$watermark-text

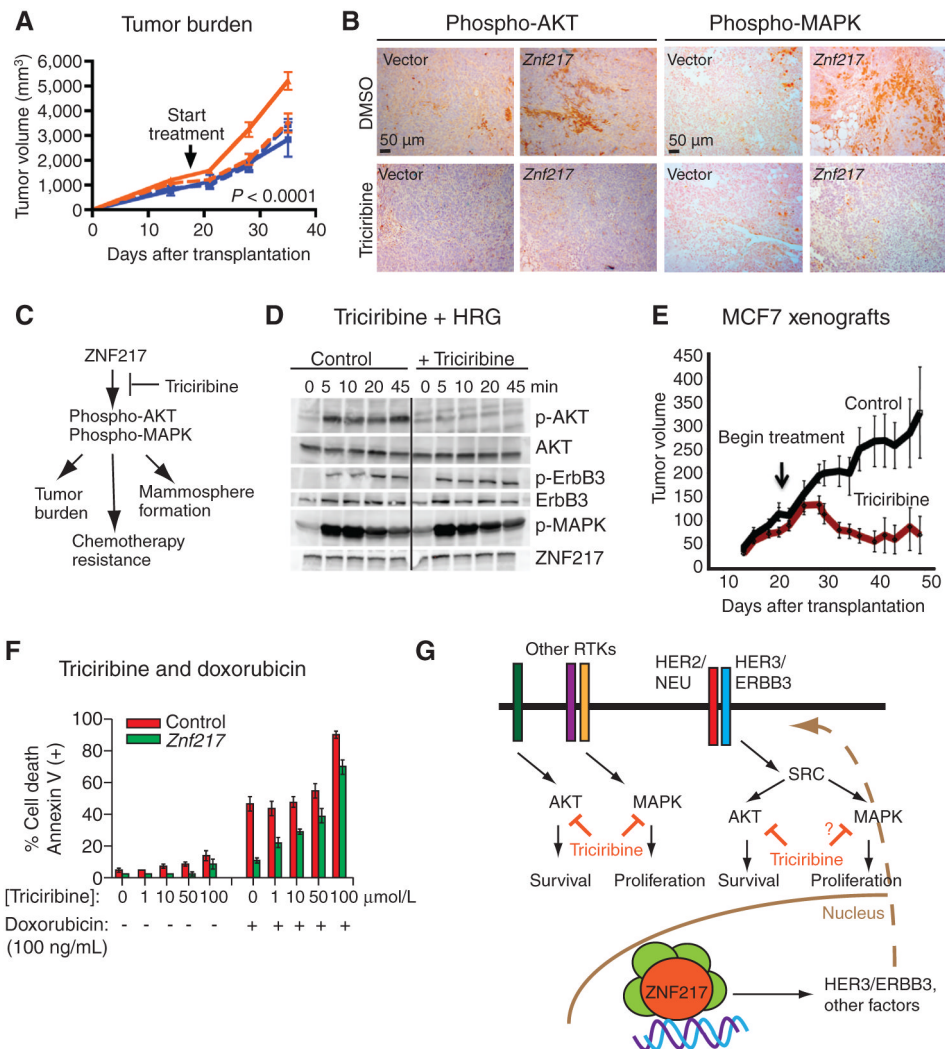


**Figure 7.** Triciribine inhibits ZNF217 *in vivo* and in human cells. **A**, tumor burden growth rate of Vo-PyMT transplants treated with dimethyl sulfoxide (DMSO) solution (solid lines) or triciribine (dotted line;  $P < 0.0001$  by genotype;  $P = 0.02$ , genotype over time; ANOVA). Vo-PyMT transplants overexpressed vector (blue) or *Znf217* (orange). Shown are the mean  $\pm$  SEM. **B**, phospho-AKT (left) and phospho-MAPK (right) protein expression by immunohistochemistry in tissues from Vo-PyMT transplants treated with either control or triciribine. **C**, model of pathways downstream from ZNF217. *Znf217* overexpression promotes phospho-AKT and phospho-MAPK. This activation is associated with increased tumor burden, chemotherapy resistance, and mammosphere formation. Triciribine can block these phenotypes of *Znf217* overexpression. **D**, MCF7 cells  $\pm$  triciribine were serum-starved overnight and stimulated with heregulin/neuregulin-1 $\beta$  for the indicated times. Cell lysates were blotted for the indicated proteins. **E**, human MCF7-M1 subcutaneous xenografts treated with control or triciribine (50 mg/kg) at the indicated time posttransplant. Ticks show mean tumor burden  $\pm$  SD. **F**, triciribine induces synthetic lethality with doxorubicin in culture. Stable HBL100 MECs (low *Znf217*, low adenosine kinase expression; *Znf217*) were treated with triciribine and doxorubicin at the indicated concentrations and monitored for cell death using Annexin V staining ( $P = 0.0002$ ; ANOVA). All doxorubicin-treated samples

were statistically different ( $P < 0.05$ ; Bonferroni posttest), whereas triciribine treatment alone did not promote statistically significant results. Graph shows mean  $\pm$  SEM. **G**, model of ZNF217 function. Increased ZNF217 promotes increased ERBB3 expression and activation of downstream signaling events during tumor progression. ZNF217 may also activate other receptor tyrosine kinases (RTK) that in turn lead to activation of AKT or MAPK pathways. *In vivo* during tumor progression, triciribine can block signaling events downstream of ZNF217 overexpression.

\$watermark-text

\$watermark-text

\$watermark-text